The Astrophysical Journal Letters, 745:L28 (5pp), 2012 February 1 doi:10.1088/2041-8205/745/2/L28

THE STRUCTURE OF THE M87 JET: A TRANSITION FROM PARABOLIC TO CONICAL STREAMLINES

Keiichi Asada[1] and Masanori Nakamura[1,2,3]
[1] Institute of Astronomy & Astrophysics, Academia Sinica, P.O. Box 23-141, Taipei 10617, Taiwan; asada@asiaa.sinica.edu.tw, nakamura@asiaa.sinica.edu.tw
[2] Department of Physics and Astronomy, The Johns Hopkins University, 3400 N. Charles Street, Baltimore, MD 21218, USA
[3] Space Telescope Science Institute, 3700 San Martin Drive, Baltimore, MD 21218, USA
Received 2011 October 6; accepted 2011 December 19; published 2012 January 11

ABSTRACT

The structure of the M87 jet, from milliarcsecond to arcsecond scales, is extensively investigated, utilizing the images taken with the European VLBI Network, MERLIN, and Very Long Baseline Array. We discover that the jet maintains a parabolic streamline over a range in size scale equal to 10^5 times the Schwarzschild radius. The jet then transitions into a conical shape farther downstream. This suggests that the magnetohydrodynamic jet is initially subjected to the confinement by the external gas which is dominated by the gravitational influence of the supermassive black hole. Afterward the jet then freely expands with a conical shape. This geometrical transition indicates that the origin of the HST-1 complex may be a consequence of the overcollimation of the jet. Our result suggests that when even higher angular resolution is provided by a future submillimeter very long baseline interferometry experiments, we will be able to explore the origin of active galactic nucleus jets.

Key words: galaxies: active – galaxies: individual (M87) – galaxies: jets

1. INTRODUCTION

M87 is one of the nearest active galaxies (16.7 Mpc; Jordán et al. 2005) that exhibits relativistic outflows. The mass of the central supermassive black hole (SMBH) is measured to be $3.2 \times 10^9\ M_\odot$ from *Hubble Space Telescope* (*HST*) observations of the ionized gas disk (e.g., Macchetto et al. 1997). Recent analyses of the stellar kinematics suggest a larger mass of $6.6 \times 10^9\ M_\odot$ (Gebhardt et al. 2011). This larger mass gives an apparent size of $\sim 8\ \mu$as for the Schwarzschild radius r_s. This galaxy therefore provides a unique opportunity to study the relativistic outflow with the highest physical resolution in units of r_s.

Based on the Very Large Array (VLA)/Very Long Baseline Interferometry (VLBI) observations during the past three decades, the structure of the M87 jet has been extensively examined. Junor et al. (1999) found a smooth variation of the jet opening angle from 60° at ∼0.03 pc to smaller than 10° over ∼10 pc, indicating that the jet is being collimated by the magnetohydrodynamic (MHD) process (Meier et al. 2001). One of the most interesting features in the M87 jet is the bright knot G, lying about 1″ (∼78 pc) from the core in the VLA maps (Owen et al. 1989). That region has been resolved by the *HST* into a structured complex known as "HST-1" (Biretta et al. 1999). It is located around 0.″8–1.″0 (or 62–78 pc) from the core. It consists of bright knots, whose (apparent) proper motions are superluminal with a range of 4*c*–6*c* (Biretta et al. 1999). A similar velocity pattern has been observed at radio frequencies using the Very Long Baseline Array (VLBA). The component of HST-1, which is the farthest upstream (i.e., HST-1d), is stationary to within the errors (<0.25*c*) and has been identified as the origin of the superluminal ejections (Cheung et al. 2007). The structure of the jet downstream of HST-1 (1″–18″ or 0.1–1.5 kpc) can be characterized by a conical shape with an opening angle of ∼6° (Owen et al. 1989). HST-1 is also a remarkable site for large flaring activity across the electromagnetic spectrum from radio through optical to X-ray bands (Madrid 2009; Harris et al. 2009). *Chandra* observations show that the flaring event started in 2000, and its brightness eventually increased more than 50 times. Peak brightness occurred in 2005 and an adiabatic compression has been suggested as a cause of the flare (Harris et al. 2006). It is thought to be one possible site for TeV γ-ray emission (Harris et al. 2009). Note that all distances are in projection throughout this section.

2. OBSERVATIONS AND DATA REDUCTIONS

2.1. EVN Data

We conducted the European VLBI Network (EVN) observations toward M87 on 2009 March 7 at a wavelength of 18 cm with the Cambridge (UK), Effelsberg (Germany), Jodrell Bank (UK), Knockin (UK), Medicina (Italy), Noto (Italy), Onsala (Sweden), Torun (Poland), and Westerbork (Netherlands) stations. Both left and right circular polarization data were recorded at each telescope using eight channels of 8 MHz bandwidth and 2 bit sampling. The data were correlated at the Joint Institute for VLBI in Europe correlator.

A priori amplitude calibration for each station was derived from a measurement of the system temperatures during each run and the antenna gain. Fringe fitting was performed using AIPS. After results of fringe fitting were applied, the data were averaged over 12 s in each intermediate frequency (IF) and self-calibrated using Difmap.

2.2. MERLIN Data

We conducted the MERLIN observations on 2007 March 9 at a wavelength of 18 cm with the Defford, Cambridge, Knockin, Darnhall, Jodrell Bank, and Tabley stations. Both left and right circular polarization data were transferred from each telescope with a 15 MHz bandwidth.

Initially, the data were pipelined, and a channel-by-channel flux scale derived from 3C 286 observation was applied. After this a priori amplitude calibration, we self-calibrated the data using Difmap.

2.3. VLBA Data

We also analyzed archival VLBA data of the M87 jet (BK073). Those observations were carried out on 2000

Table 1
Qualities of the Images

Observation	Synthesized Beam			Peak Intensity	rms Noise Level	Dynamic Range
	(mas)	(mas)	(deg)	(Jy beam^{-1})	(mJy beam^{-1})	
EVN	17.8	13.1	76.1	1.77	0.47	3770
MERLIN	25	25	0°	2.00	1.21	1650
VLBA	1.22	0.59	−3.99	0.838	0.15	5590

January 22 at 15 GHz with all ten stations of the VLBA and one station of the VLA. Four IFs, each with an 8 MHz bandwidth, were recorded at each telescope. Data reduction was conducted in the same manner as for the EVN observations. We reproduced an M87 image, which is consistent with that published in Kovalev et al. (2007).

3. RESULTS

We show the images from EVN, MERLIN, and VLBA observations in Figure 1. Image qualities are summarized in Table 1. The bright core at the eastern edge of the jet and continuous jet emission are detected in all images. We define the core with a Gaussian model that was fitted to the innermost bright region in all the images. The isolated component at the distance of 900 mas from the core in the EVN image is the HST-1 knot. It corresponds to the first bright component to the west of the core in the MERLIN image. This feature was not detected in the VLBA image at 15 GHz, since those data were taken before the HST-1 component underwent its flaring event. One of the most important achievements in our observations is a clear detection of continuous jet emission up to 500 mas from the core in the EVN image. The continuous jet structure between 160 and 500 mas has been suggested in previous measurements (Reid et al. 1989; Cheung et al. 2007), but here they are robustly detected and resolved with high significance in our EVN observations.

In order to illustrate the structure of the M87 jet, we analyze the jet emission along a position angle of 338° and fit the cross sections of the jet with one Gaussian or multiple Gaussians for all the images. We define the width of the jet as the deconvolved FWHM for the one-Gaussian fitting case. For the multiple-Gaussian fitting case, we define the distance between the outer edges of the FWHMs as the width of the jet. We note that the jet cross sections can be represented mainly by two Gaussians when multiple Gaussians were fitted. This is consistent with the edge-brightened model suggested by previous observations (Owen et al. 1989; Reid et al. 1989; Junor et al. 1999).

We show the radius of the jet as a function of the deprojected distance from the core in units of r_s in Figure 2. Note that the radius as defined perpendicular to the jet does not suffer from orientation effects. We assume that the viewing angle of the jet is 14° based on a beaming analysis (Wang & Zhou 2009). Hereafter, we use the deprojected distance along the jet throughout the paper. We note that 1 mas corresponds to 530 r_s in deprojected distance. We measure the radius of the jet at the innermost region by using the previous VLBA image at 43 GHz by Walker et al. (2008) as well. The jet radius increases downstream, as clearly shown in Figure 2. We found that the streamlines of the M87 jet can be divided into two different regimes: (1) a parabolic shape with $a = 1.73 \pm 0.05$ ($z \propto r^a$, where r is the radius of the jet emission and z is the axial distance from the core), on scales up to $\sim 2.5 \times 10^5$ r_s, and (2) a conical shape with $a = 0.96 \pm 0.1$ starting at around

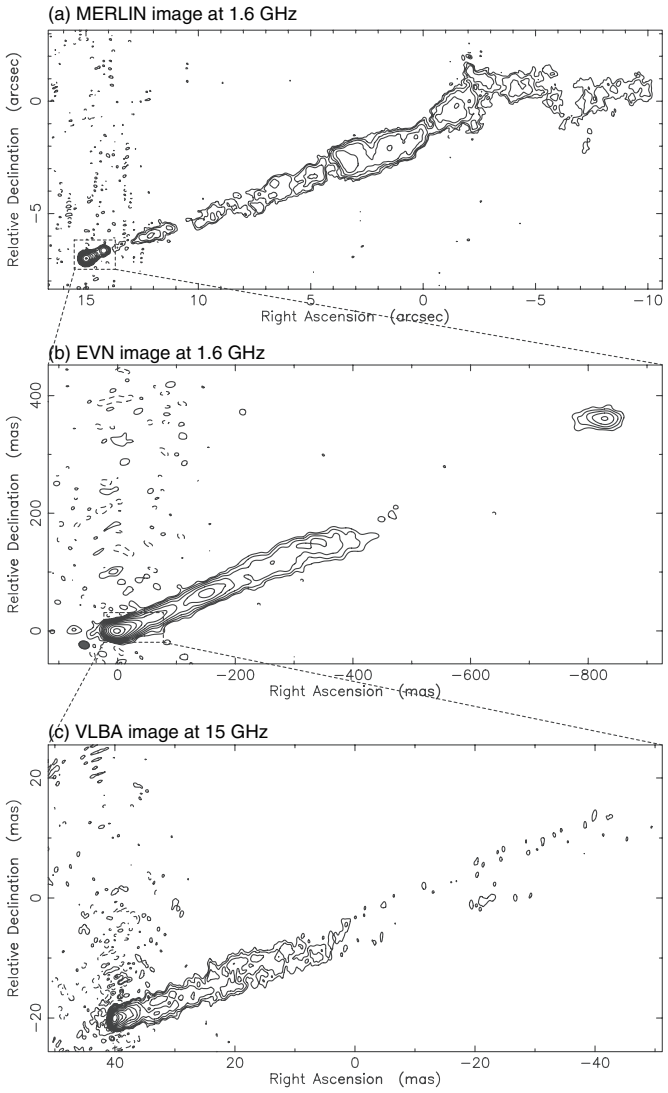

Figure 1. (a) MERLIN image of M87. Contours are plotted at −1, 1, 2, ... , 1024 × 3.64 mJy beam^{-1}, which is three times the residual rms noise. The image is restored with a circular beam of 25 arcsec to emphasize the extended structure. (b) EVN image of M87. Contours are plotted at −1, 1, 2, ... , 1024 × 1.37 mJy beam^{-1}, which is three times the residual rms noise. The synthesized beam is 17.8 mas × 13.1 mas with the major axis at a position angle of 76.1. (c) VLBA image of M87. Contours are plotted at −1, 1, 2, ... , 1024 × 0.45 mJy beam^{-1}, which is three times the residual rms noise. The synthesized beam is 1.22 mas × 0.59 mas with the major axis at a position angle of −3.99.

2.5×10^5 r_s. It is remarkable that the jet propagates with a single power-law streamline over more than three orders of magnitude in distance. Furthermore, it is notable that the two observed power-law streamlines intersect at 2×10^5 r_s, which is close to the Bondi radius of 3.8×10^5 r_s (∼250 pc)[4] (Allen et al.

[4] The original value is replaced taking into account the mass difference of SMBH.

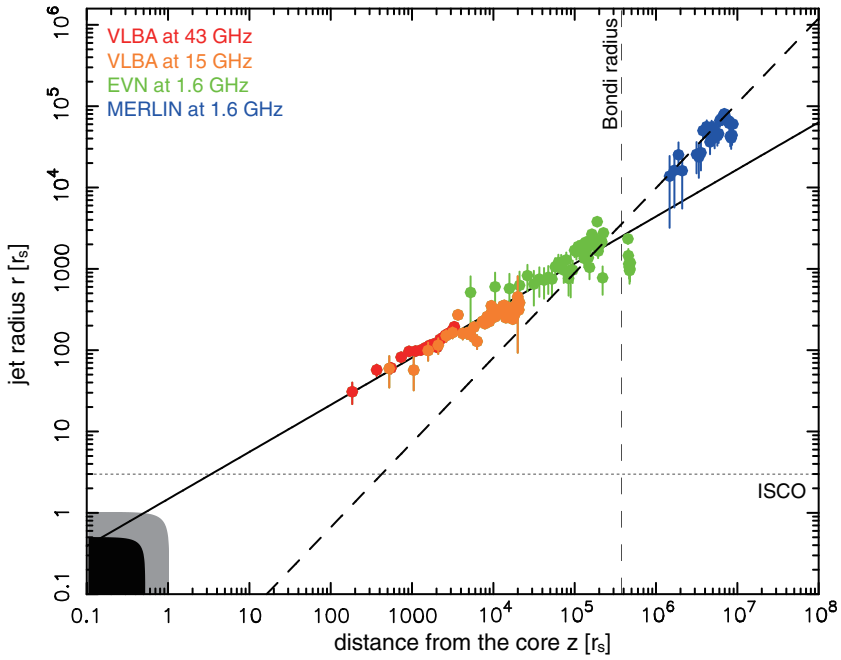

Figure 2. Distribution of the radius of the jet as a function of the deprojected distance from the core in units of r_s. We used images obtained by previous VLBA measurements at 43 GHz (red circles) and at 15 GHz (orange circles), EVN measurements at 1.6 GHz (green circles), and MERLIN measurements at 1.6 GHz (blue circles). The jet is described by two different shapes. The solid line indicates a parabolic structure with a power-law index a of 1.7, while the dashed line indicates a conical structure with a of 1.0. HST-1 is located around 5×10^5 r_s. The black area shows the size of the minor axis of the event horizon of the spinning black hole with maximum spin. The gray area indicates the size of the major axis of the event horizon of the spinning black hole with maximum spin, and corresponds to the size of the event horizon of the Schwarzschild black hole. The dotted line indicates the size of the inner stable circular orbit (ISCO) of the accretion disk for the Schwarzschild black hole.

2006). Indeed, this is the first observational evidence detecting a transition from parabolic to conical streamlines in extragalactic jet systems.

4. DISCUSSION AND SUMMARY

4.1. Unconfined Structure: Downstream of HST-1

We consider a conical streamline ($z \propto r^a, a = 1$) for supersonic jets. In an adiabatic jet, the internal pressure $p_{\rm jet}$ decreases with the axial distance z as $z^{-2\Gamma}$ (Γ: the ratio of specific heats). So, we speculate that the constant expansion of the jet radius and a conical structure downstream of HST-1 to knot A in the M87 jet require the same axial gradient for the external interstellar medium (ISM) pressure, $p_{\rm ism}$, as $p_{\rm jet}$ (Owen et al. 1989). If $p_{\rm ism}$ decreases slower than $p_{\rm jet}$, then $p_{\rm ism} > p_{\rm jet}$ at some distance so that a recollimation shock will be triggered (Sanders 1983). The self-similar solution of a conical streamline for the magnetized case (with a purely toroidal field component) requires $p_{\rm ism} \propto z^{-b}, b = 4$ (Zakamska et al. 2008). For a general (non-self-similar) case, $b > 2$ is allowed in analytical and numerical models (Tchekhovskoy et al. 2008; Lyubarsky 2009; Komissarov et al. 2009). X-ray observations reveal the ISM properties such as the Bondi radius $r_{\rm B} \sim 250$ pc and the King core radius $r_{\rm c} \simeq 1.4$ kpc (see, e.g., Young et al. 2002; Di Matteo et al. 2003; Allen et al. 2006). Thus, the region of conical streamlines in the M87 jet lies between $r_{\rm B}$ and the marginal radius for the power-law decay beyond $r_{\rm c}$ in the King profile, indicating that the ISM distribution is essentially uniform. We thus rule out that the structure downstream of HST-1 is hydrostatically confined by $p_{\rm ism}$ in order to conform to a conical streamline.

In order to possess a conical streamline without any overcollimation between knots HST-1 and A, the condition $p_{\rm jet} \gtrsim p_{\rm ism}$ should be maintained. Knots HST-1 to A do appear to be overpressured with respect to the external pressure (Owen et al. 1989). However, the $p_{\rm jet}$ of the inter-knot regions, as estimated by the minimum energy argument for the VLA data (Sparks et al. 1996), appears underpressured with respect to $p_{\rm ism}$, as estimated by the recent X-ray observations (Young et al. 2002; Rafferty et al. 2006). One possibility is an underestimation of the magnetic field strength when the toroidal (azimuthal) components are not considered (cf. Owen et al. 1989). It has been further suggested that the magnetic field energy is at least in equipartition (or even larger with a factor of 1–2) with the energy of the radiating ultrarelativistic electrons (Stawarz et al. 2005).

We note that overpressured knots do appear to have trails of stationary recollimation shocks in purely hydrodynamic jets. Falle & Wilson (1985) performed hydrodynamic simulations to apply stationary recollimation shocks to the observed knots at VLA scales under the assumption of the shallow ISM gradient ($p_{\rm ism} \propto z^{-1}$). Stationary features, however, are in conflict with the observed large proper motions (Biretta et al. 1995, 1999), while the ISM also does not appear to have such a gradient. Therefore, we suggest that the highly magnetized nature of the jet may be responsible for the conical part of the M87 jet.

4.2. Confined Structure: Upstream of HST-1

We next consider a parabolic streamline ($1 < a \leqslant 2$) for supersonic jets. It is shown that the magnetized jet can be parabolic in analytical and numerical models where the ISM pressure is decreasing as $p_{\rm ism} \propto z^{-b}, b = 2$ (Tchekhovskoy et al. 2008; Komissarov et al. 2009). A self-similar solution also exists for non-magnetized cases with a pure parabolic streamline ($a = 2$) under the same $p_{\rm ism}$ dependence with $b = 2$ (Zakamska et al. 2008). Their solution indicates $p_{\rm jet} \lesssim p_{\rm ism}$ with pressure

increasing near the jet edge. So far, no analytical or numerical solutions, except $a = 2$, have been derived in the non-magnetized cases. We note that even in a hydrodynamic recollimation shock model, the jet boundary ("shocked zone" at the interface of the jet and the ISM) is expected to be parabolic. However, the ISM is required to be *uniform* ($p_{\rm ism} \sim$ const.; Komissarov & Falle 1997; Nalewajko & Sikora 2009).

In order to have parabolic streamlines, $b \sim 2$ is required in magnetized jets. It is important to examine the distributions of $p_{\rm ism}$. A recent analytical model for a giant advection-dominated accretion flow (Narayan & Fabian 2011) shows $b \sim 2.3$ from beyond $r_{\rm B}$ down to the SMBH, and it is universally derived for slow rotation of the ISM ($\lesssim$30% of the Keplerian speed) with the wider range of the α-viscosity parameter (0.001–0.3; Shakura & Sunyaev 1973). A spherically symmetric accretion with MHD turbulence (Shcherbakov 2008) produces $b \sim 2.1$ without a strong dependence on the parameters and the equation of state. However, the spatial resolution in current X-ray observations is not high enough to resolve this region.

4.3. HST-1

The radius of HST-1 appears to be smaller than the size estimated by the two power-law streamlines. The maximum measured radius of the HST-1 region is $2200\,r_s \pm 300\,r_s$ and the mean value is $1300\,r_s \pm 150\,r_s$, while the expected radii are $3000\,r_s \pm 400\,r_s$ for the parabolic case and $4100\,r_s \pm 200\,r_s$ for the conical case, respectively. One possibility is that the jet is subjected to overcollimation toward HST-1.

As is seen in Figure 2, HST-1 is located downstream of the Bondi radius ($r_{\rm B}$), where the jet changes from a parabolic to a conical shape. This transition is presumably caused by the different profiles of the external pressure (changing from steep to shallow gradients). The distribution of the external gas follows the influence of gravity from the central SMBH inside of $r_{\rm B}$, while it can be flattened outside of $r_{\rm B}$. The field strength $|\boldsymbol{B}|$ at HST-1 is 0.5–20 mG as estimated by the X-ray variability (Perlman et al. 2003; Harris et al. 2009). Supposing $|\boldsymbol{B}| \sim$ 1 mG for our reference, the magnetic pressure is expected to be about 100 times larger (i.e., overpressured) than the ISM value $p_{\rm ism} \sim 4.3 \times 10^{-10}$ dyn cm^{-2} (Allen et al. 2006; $n_e = 0.17$ cm^{-3} and $kT = 0.8$ KeV).

Another interesting objective is to understand the production of the superluminal components (Biretta et al. 1999; Cheung et al. 2007). The observed motions are modeled by the quad relativistic shocks in the MHD helical jet (Nakamura et al. 2010). Recent optical polarimetry requires a coherent helical field to explain the distribution of polarization vectors (perpendicular to the jet; Perlman et al. 2003) and variations of the radio electric vector positional angles as well as the fractional polarization degree (Chen et al. 2011), indicating either a helical distortion to the jet or a shock propagating through a helical jet (Perlman et al. 2011).

An interpretation for the origin of HST-1 as a hydrodynamic recollimation shock has been proposed by Stawarz et al. (2006, hereafter S06) and Bromberg & Levinson (2009, hereafter BL09). S06 do not explain the observed gradual collimation and are inconsistent with our observational result. They assume a freely expanding (i.e., a conical) jet which is already in the particle-dominated regime upstream of HST-1. S06 suggest a shallow external pressure profile $p_{\rm ism} \propto z^{-0.6}$ inside some critical radius of 3″ (≈234 pc), as determined by a stellar cusp (a break in the stellar surface brightness of the M87 host galaxy; Lauer et al. 1992). BL09 also model the recollimation shock at HST-1 with the same pressure profile.

In summary, we propose that a transition from parabolic to conical streamlines occurs via a strong compression due to the change in the slope of the axial profile of $p_{\rm ism}$. This condition can be achieved by an imbalance between $p_{\rm jet}$ and $p_{\rm ism}$ in the radial direction due to the overcollimation. It is remarkable that recent general relativistic MHD simulations (McKinney 2006) reproduce the observed transition from parabolic ($a \sim 1.7$) to conical ($a \sim 1.0$) streamlines. However, the scale of the transition does not match with the observations. We suggest that the properties of MHD jets should be considered in a realistic ISM environment.

4.4. Toward the Jet Origin: BH or Disk?

Recent VLBA observations indicate that the VLBI core at 43 GHz (core$_{43}$) is located at $20\,r_s$ from the position of the SMBH for the viewing angle of 14° (Hada et al. 2011). With the VLBA image, the size of core$_{43}$ can be measured to be $17 \pm 4\,r_s$ at a position angle of 68°, which is approximately perpendicular to the jet axis. If we assume that the core is the innermost part of the jet emission, the radius of the jet is $9 \pm 2\,r_s$. This is in good agreement with the extrapolated radius of the jet of $9 \pm 2\,r_s$ assuming parabolic streamlines in the inner region. If this is the case, the jet propagates with a single power-law streamline over more than four orders of magnitude of distance.

The jet opening angle is one of the key parameters in the MHD jet acceleration mechanism. Blandford & Payne (1982, hereafter BP82) suggest that the jet is initiated by the magneto-centrifugal force if the jet inclination angle between the penetrating magnetic line of force and the accretion disk is smaller than 60°, which corresponds to a jet opening angle larger than 60°. If we assume that core$_{43}$ is the innermost part of jet emission, the jet opening angle would be estimated to be 46° at $20\,r_s$. Therefore, core$_{43}$ would be located downstream of the Alfvén surface where the magnetic pressure gradient force plays a role. Thus, future submillimeter VLBI projects can access initial acceleration mechanisms by direct imaging and measure the deviation from parabolic streamlines upstream of core$_{43}$.

Furthermore, as we show in Figure 2, the parabolic jet can be extrapolated to the vicinity of the SMBH. At the "axial" distance of $z = 3.4\,r_s$ from the SMBH, it intersects the theoretically expected inner stable circular orbit (ISCO) of the accretion disk for a Schwarzschild black hole. If the jet radius departs from the extrapolation line well beyond $3.4\,r_s$, it will indicate that the jet originates in the accretion disk (BP82). If the streamline is as extrapolated down to $3.4\,r_s$, the jet must originate from the accretion disk (BP82) around a spinning black hole and/or the ergosphere of the spinning black hole (Blandford & Znajek 1977, hereafter BZ77). If we see no departure down to $0.5\,r_s$ from the SMBH, it indicates that the jet originates from the ergosphere of the spinning black hole (BZ77). Note the above discussion for prograde spinning black holes, while the upper limit of the ISCO is $4.5\,r_s$ for retrograde spinning black holes. Therefore, tracing back the ridge line and identifying the ejection point of the jet is one of the crucial tests to an evaluation of the formation mechanism of the jet (BP82 and/or BZ77). More fundamentally, it provides an important method for detection of the spin of the SMBH[5] and evaluation

[5] It is also interesting to compare with the jet power as predicted by Garofalo et al. (2010).

of the general theory of relativity. Such conjectures will be explored by direct imaging with future submillimeter VLBI experiments.

We thank M. Inoue, A. Doi, H. Nagai, D. Garofalo, and P. T. P. Ho for stimulating discussions and proof reading. We sincerely acknowledge R. Craig Walker for providing the VLBA image at 43 GHz. M.N. is grateful to D. L. Meier and C. A. Norman for inspiring discussions. M.N. was supported by the Allan C. Davis Fellowship jointly awarded by JHU and STScI. The European VLBI Network is a joint facility of European, Chinese, South African, and other radio astronomy institutes funded by their national research councils. MERLIN is a National Facility operated by the University of Manchester at Jodrell Bank Observatory on behalf of STFC. The National Radio Astronomy Observatory is a facility of the National Science Foundation operated under cooperative agreement by Associated Universities, Inc.

Facilities: EVN, MERLIN, VLBA

REFERENCES

Allen, S. W., Dunn, R. J. H., Fabian, A. C., Taylor, G. B., & Reynolds, C. S. 2006, MNRAS, 372, 21
Biretta, J. A., Sparks, W. B., & Macchetto, F. 1999, ApJ, 520, 621
Biretta, J. A., Zhou, F., & Owen, F. N. 1995, ApJ, 447, 582
Blandford, R. D., & Payne, D. G. 1982, MNRAS, 199, 883
Blandford, R. D., & Znajek, R. L. 1977, MNRAS, 179, 433
Bromberg, O., & Levinson, A. 2009, ApJ, 699, 1274
Chen, Y. J., Zhao, G.-Y., & Shen, Z.-Q. 2011, MNRAS, 416, L109
Cheung, C. C., Harris, D. E., & Stawarz, Ł. 2007, ApJ, 663, L65
Di Matteo, T., Allen, S. W., Fabian, A. C., Wilson, A. S., & Young, A. J. 2003, ApJ, 582, 133
Falle, S. A. E. G., & Wilson, M. J. 1985, MNRAS, 216, 79
Garofalo, D., Evans, D. A., & Sambruna, R. M. 2010, MNRAS, 406, 975
Gebhardt, K., Adams, J., Richstone, D., et al. 2011, ApJ, 729, 119
Hada, K., Doi, A., Kino, M., et al. 2011, Nature, 477, 185
Harris, D. E., Cheung, C. C., Biretta, J. A., et al. 2006, ApJ, 640, 211
Harris, D. E., Cheung, C. C., Stawarz, Ł., Biretta, J. A., & Perlman, E. S. 2009, ApJ, 699, 305
Jordán, A., Côté, P., Blakeslee, J. P., et al. 2005, ApJ, 634, 1002
Junor, W., Biretta, J. A., & Livio, M. 1999, Nature, 401, 891
Komissarov, S. S., & Falle, S. A. E. G. 1997, MNRAS, 288, 833
Komissarov, S. S., Vlahakis, N., Königl, A., & Barkov, M. V. 2009, MNRAS, 394, 1182
Kovalev, Y. Y., Lister, M. L., Homan, D. C., & Kellermann, K. I. 2007, ApJ, 668, L27
Lauer, T., Faber, S. M., Lynds, R. C., et al. 1992, AJ, 103, 703
Lyubarsky, Y. 2009, ApJ, 698, 1570
Macchetto, F., Marconi, A., Axon, D. J., et al. 1997, ApJ, 489, 579
Madrid, J. P. 2009, AJ, 137, 3864
McKinney, J. C. 2006, MNRAS, 368, 1561
Meier, D. L., Koide, S., & Uchida, Y. 2001, Science, 291, 84
Nakamura, M., Garofalo, D., & Meier, D. L. 2010, ApJ, 721, 1783
Nalewajko, K., & Sikora, M. 2009, MNRAS, 392, 1205
Narayan, R., & Fabian, A. C. 2011, MNRAS, 415, 3721
Owen, F. N., Hardee, P. E., & Cornwell, T. J. 1989, ApJ, 340, 698
Perlman, E. S., Adams, S. C., Cara, M., et al. 2011, ApJ, 743, 119
Perlman, E. S., Harris, D. E., Biretta, J. A., Sparks, W. B., & Macchetto, F. D. 2003, ApJ, 599, L65
Rafferty, D. A., McNamara, B. R., Nulsen, P. E. J., & Wise, M. W. 2006, ApJ, 652, 216
Reid, M. J., Biretta, J. A., Junor, W., Muxlow, T. W. B., & Spencer, R. E. 1989, ApJ, 336, 112
Sanders, R. H. 1983, ApJ, 266, 73
Shakura, N. I., & Sunyaev, R. A. 1973, A&A, 24, 337
Shcherbakov, R. V. 2008, ApJS, 177, 493
Sparks, W. B., Biretta, J. A., & Macchetto, F. 1996, ApJ, 473, 254
Stawarz, Ł., Aharonian, F., Kataoka, J., et al. 2006, MNRAS, 370, 981
Stawarz, Ł., Siemiginowska, A., Ostrowski, M., & Sikora, M. 2005, ApJ, 626, 120
Tchekhovskoy, A., McKinney, J. C., & Narayan, R. 2008, MNRAS, 388, 551
Walker, R. C., Ly, C., Junor, W., & Hardee, P. J. 2008, J. Phys.: Conf. Ser., 131, 012053
Wang, C.-C., & Zhou, H.-Y. 2009, MNRAS, 395, 301
Young, A. J., Wilson, A. S., & Mundell, C. G. 2002, ApJ, 579, 560
Zakamska, N. L., Begelman, M. C., & Blandford, R. D. 2008, ApJ, 679, 990